



Quantifying the spatiotemporal influence of acute myocardial ischemia on volumetric conduction velocity

Wilson W. Good^{a,b,c,*}, Brian Zenger^{a,b,c,d}, Jake A. Bergquist^{a,b,c}, Lindsay C. Rupp^{a,b}, Karli K. Gillette^e, Matthias A.F. Gsell^e, Gernot Plank^e, Rob S. MacLeod^{a,b,c}

^a Scientific Computing and Imaging Institute, University of Utah, Salt Lake City, UT, USA

^b Department of Biomedical Engineering, University of Utah, Salt Lake City, UT, USA

^c Nora Eccles Cardiovascular Research and Training Institute, University of Utah, Salt Lake City, UT, USA

^d School of Medicine, University of Utah, Salt Lake City, UT, USA

^e Medical University of Graz, Graz, Austria

ARTICLE INFO

Available online xxxx

Keywords:

Volumetric conduction velocity

Acute ischemia

Biphasic conduction velocity

Wave refraction

ABSTRACT

Introduction: Acute myocardial ischemia occurs when coronary perfusion to the heart is inadequate, which can perturb the highly organized electrical activation of the heart and can result in adverse cardiac events including sudden cardiac death. Ischemia is known to influence the ST and repolarization phases of the ECG, but it also has a marked effect on propagation (QRS); however, studies investigating propagation during ischemia have been limited.

Methods: We estimated conduction velocity (CV) and ischemic stress prior to and throughout 20 episodes of experimentally induced ischemia in order to quantify the progression and correlation of volumetric conduction changes during ischemia. To estimate volumetric CV, we 1) reconstructed the activation wavefront; 2) calculated the elementwise gradient to approximate propagation direction; and 3) estimated conduction speed (CS) with an inverse-gradient technique.

Results: We found that acute ischemia induces significant conduction slowing, reducing the global median speed by 20 cm/s. We observed a biphasic response in CS (acceleration then deceleration) early in some ischemic episodes. Furthermore, we noted a high temporal correlation between ST-segment changes and CS slowing; however, when comparing these changes over space, we found only moderate correlation (corr. = 0.60).

Discussion: This study is the first to report volumetric CS changes (acceleration and slowing) during episodes of acute ischemia in the whole heart. We showed that while CS changes progress in a similar time course to ischemic stress (measured by ST-segment shifts), the spatial overlap is complex and variable, showing extreme conduction slowing both in and around regions experiencing severe ischemia.

© 2021 Elsevier Inc. All rights reserved.

Introduction

Electrical propagation of the depolarization wavefront through the heart is a complex but ordered phenomena and changes to this propagation, such as during acute myocardial ischemia, have long been thought to result in sudden cardiac death and other adverse cardiac events [1,2]. Myocardial ischemia occurs when coronary perfusion to the heart is inadequate, initiating an electrochemical cascade known to influence the ST and repolarization phases of the ECG, but it also has a marked effect on electrical depolarization (QRS) [3]. Interestingly, while changes to propagation have been studied during episodes of ischemia, these have been limited to surface based measurements.

Moreover, there have been few reports to characterize the degree of correlation between these propagation changes and the regions of ischemic stress. This paucity of investigation may be explained by the difficulty of achieving high-resolution sampling of the activation sequence within the myocardial volume. Such high-resolution intramural sampling is necessary to capture the complex spread of activation even under control conditions; it is just as necessary but even more challenging during ischemic stress.

The electrical signature of ischemic stress has been studied extensively since the advent of electrocardiography, emphasizing ST segment changes as indicative of underlying ischemic stress [4–7]. Our previous studies have also used changes in the ST-segment to estimate, detect, and delineate regions of ischemic stress, by means of both epicardial and intramyocardial measurements [4–7]. The goal of the present study was to measure ST-segment changes and compare them with conduction velocities, estimated using newly developed techniques [8]

* Corresponding author at: Scientific Computing and Imaging Institute, University of Utah, Salt Lake City, UT, USA.

E-mail address: wgood@sci.utah.edu (W.W. Good).

to explore the spatiotemporal relationship between ischemic stress and changes in propagation.

Changes in propagation during periods of ischemic stress are thought to underpin many of the arrhythmogenic mechanisms long associated with ischemia; however, the lack of investigations in intramural propagation has prevented consensus [1,6,7,9]. Estimation of cardiac conduction velocity is performed during mapping studies from spatially distributed measurements, and the majority of published studies have been limited to surface-based measurements and, subsequently, surface-based estimations of CV [9–13]. In a recent study, we examined the differences between the CV estimated on the epicardium and from within the heart and found that the magnitude of CV determined from epicardial measurements will be systematically overestimated [8]. This overestimation was consistent across parameters such as pacing site, cardiac geometry, and the technique used to estimate CV, highlighting the necessity of volume-based measurements to study propagation. Furthermore, studying intramural propagation allows us to evaluate transmural heterogeneity of CV and how it is influenced spatially by ischemic stress. Here we applied our recently validated intramyocardial estimations of CV⁸ to extend our understanding of propagation changes during acute ischemia.

The goal of this study was to examine the spatiotemporal relationship between the intramural development of ST-segment shifts and changes in CV during acute ischemia. We examined how CV changed in the presence of ischemic stress by measuring it throughout episodes of induced, controlled acute ischemia. Since ischemia affected both components of CV independently, we report effects on the directionality of the wavefront as well as the magnitude of the velocity, which we refer to as ‘conduction speed’ (CS). We also examined the correlation of ischemic stress and CS over time and space. We identified high temporal correlations between ischemic stress and CS slowing. Less anticipated were the complex spatial relationships we documented between CS slowing in and around regions of ischemic stress that resulted in low spatiotemporal correlation (STC). We also observed a biphasic response in the conduction speed changes, which we found to be predominately isolated to the endocardium.

Methods

Experimental preparation and model generation

Signals were acquired from 20 episodes of ischemia captured across four in situ canine experiments [4,5]. All experiments were performed under deep anesthesia using procedures approved by the Institutional Animal Care and Use Committee of the University of Utah and conforming to the Guide for the Care and Use of Laboratory Animals (protocol number 17-04016 approved on 05/17/2017). Details of the experimental preparation, such as the induction and grading of ischemia, have been described previously [4,14,15]. Briefly, acute and reversible ischemia was induced via a supply-demand mismatch in the tissue perfused by the left anterior descending (LAD) coronary artery. The flow rate through the LAD was modulated via a hydraulic occluder placed around the artery while the heart rate was controlled by electrically stimulating the right atrium. Each ischemic episode lasted 7–16 min with a 30-min recovery period between episodes to allow the heart to return to baseline conditions.

To record the extracellular potentials within the myocardium, we inserted 12–25 intramural needles, each containing 10 unipolar electrodes spaced at 1.5–1.8 mm, into the putative perfusion bed [4]. Fig. 1A shows a schematic of such a needle. Spacing between adjacent needles was 1–2 cm, depending on the experimental preparation. We defined the region outlined by the needle electrodes as the ‘needle envelope’. Fig. 1C shows an example of such a needle envelope. We acquired electrograms from all needle electrodes simultaneously, either continuously or in ‘runs’ of 3–6 s duration in 15 s intervals. Continuous runs were later segmented for analysis. Representative beats used in

this analysis were isolated, baseline corrected, filtered, and fiducialized using the PFEIFER open source platform [16].

We implemented an image-based modeling pipeline in order to facilitate the generation of geometric models of hearts from each experiment, which became the basis for estimation of conduction velocity. To compare across experiments, we expressed the models in ‘universal ventricular coordinates’ (UVCs), a system developed for the CARPentry framework that uses anatomical features to align each heart into a common coordinate system [17]. The hearts were removed at the end of each experiment and imaged using a dedicated small-animal MRI system to acquire high-resolution three-dimensional scans. We then used semi-automated tools in our open-source Seg3D system (www.seg3d.org) to create subject-specific segmentations, which included locations of the needle electrodes; these segmentations formed the basis of tetrahedral meshes with an approximate edge length of 650 μm constructed using our meshing tool, Cleaver (<https://www.sci.utah.edu/cibc-software/cleaver.html>) [4,18,19]. The transmural (ρ) UVC coordinates provided simple stratification of the ventricular mesh into subendocardial ($0 \leq \rho \leq 0.33$), midmyocardial ($0.33 > \rho \leq 0.66$), and the subepicardial ($0.66 < \rho \leq 1.0$) regions. Fig. 1C visualizes the ρ coordinate values in UVC space.

Estimating volumetric conduction velocity and ischemia

To estimate volumetric CV, we 1) used a radial basis interpolation method to reconstruct the activation wavefront from measured values (activation time was determined using the min dV/dt technique [16]) throughout the mesh [20]; 2) calculated the elementwise gradient of activation time to approximate propagation direction; and 3) estimated CV with an inverse-gradient technique [10,11,20,21]. In a recent study, we showed that the level of sampling used in our experiments is adequate to reconstruct the wavefront with high fidelity [20]. Fig. 2A shows an example of activation times distributed throughout the needle envelope during an ischemic episode. We then estimated the wavefront direction by calculating the direction of the gradient of ATs in each element of the needle envelope and then inverting and taking its partial derivative [10,20]. The result is a CV vector assigned to each element in the geometric model from which we computed elementwise conduction speed (CS) as the scalar magnitude of the CV vector. Fig. 2B shows an example of estimated volumetric CV.

Quantifying wavefront refraction

To measure the change in direction of the wavefront, we quantified ‘wavefront refraction’ (WR), as an analog to the refraction of light. We defined refraction as the elementwise angle between the CV at the beginning of the episode with that from each subsequent run. The result was an angle of refraction in each element for each run. Fig. 2C shows the spatiotemporal development of WR throughout an ischemic episode.

Quantifying ischemic stress

We estimated the spatial extent of ischemia using an approach detailed in previous studies [4,20]. Briefly, values of ST40% were determined from the potential at a time point 40% between the end of the QRS and the peak of the T wave, as determined by the RMS signal created from all electrograms [5]. The measured values were interpolated into the entire needle envelope. The value of ST40% was used as a surrogate for ischemic stress and to demarcate its spatial distribution. Fig. 2D shows an example of the spatiotemporal development of ST40% throughout an ischemic episode.

Correlation between the progression of ST40% and conduction speed

Temporal correlation between the progression of ischemic stress and conduction speed change

To determine the temporal relationship between CS changes and ST40% development, we measured their correlation over time.

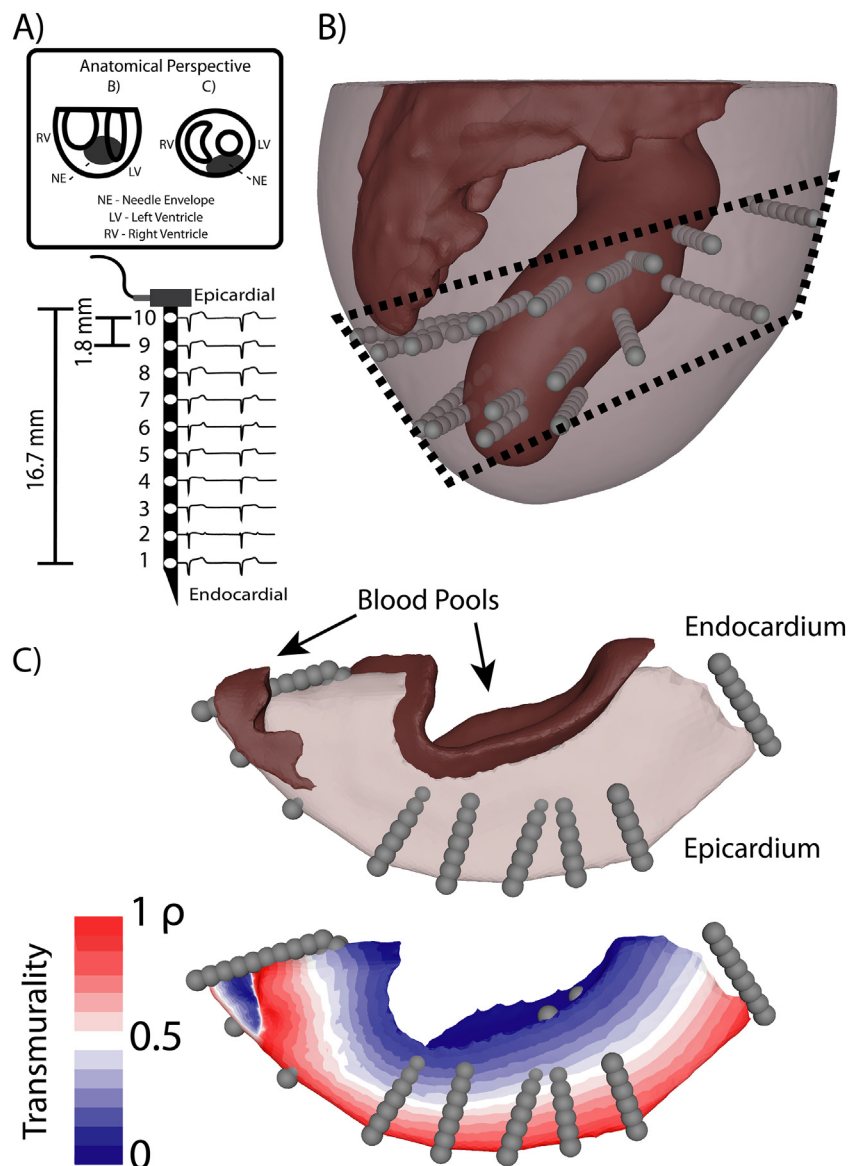


Fig. 1. A visualization of the intramural needle distribution within the myocardium. **A)** Top: a schematic representing the anatomical perspective in images B) and C). Bottom: Schematic representation of the intramural needle with example intramural signals. **B)** Image-based mesh of the cardiac ventricles with intramural needles (gray spheres) **C)** Top: Needle envelope from the superior perspective. Bottom: Needle envelope with the transmural (ρ) coordinate.

We first integrated across space by computing the median values of ST40% and CS across all nodes, and generated a single, global value for each beat. The resulting time signals capture the progression of the global values (ST40% or CS) over a single ischemic episode and we refer to them as ‘run-metrics’ [20] (e.g., Fig. 5B). Each run-metric was normalized to range from 0 to 1. Because CS changes are predominately negative, i.e., conduction slows with ischemia, we negated the CS run-metric and refer to ‘conduction slowing’.

Spatiotemporal correlation between progression of ischemic stress and conduction speed change

In addition to temporal correlation of ST40% and CS, we evaluated their correlation over space and time, which we refer to as ‘spatiotemporal correlation’ (STC). For this analysis, we once again performed a temporal correlation, but in this case of the elementwise run-metrics, which resulted in a temporal correlation for each element. We evaluated the median STC over all elements as a global comparison and

then binned the elements by their transmural extent and found the medians of the resulting distributions.

Characterizing the biphasic response in conduction speed

We observed a biphasic response in the progression of conduction speed, i.e., a transient increase followed by reduction, which has been observed in previous studies and we characterized the magnitude and duration of this change. We also wanted to characterize the time points at which we beginning to see morphological changes to ST40% and CS and therefore determined the median time at which these changes occurred across all episodes. We observed a biphasic response in 12 of the 20 episodes of ischemia and restricted our characterization to these episodes. To characterize the biphasic response, we measured its temporal width and the peak amplitude.

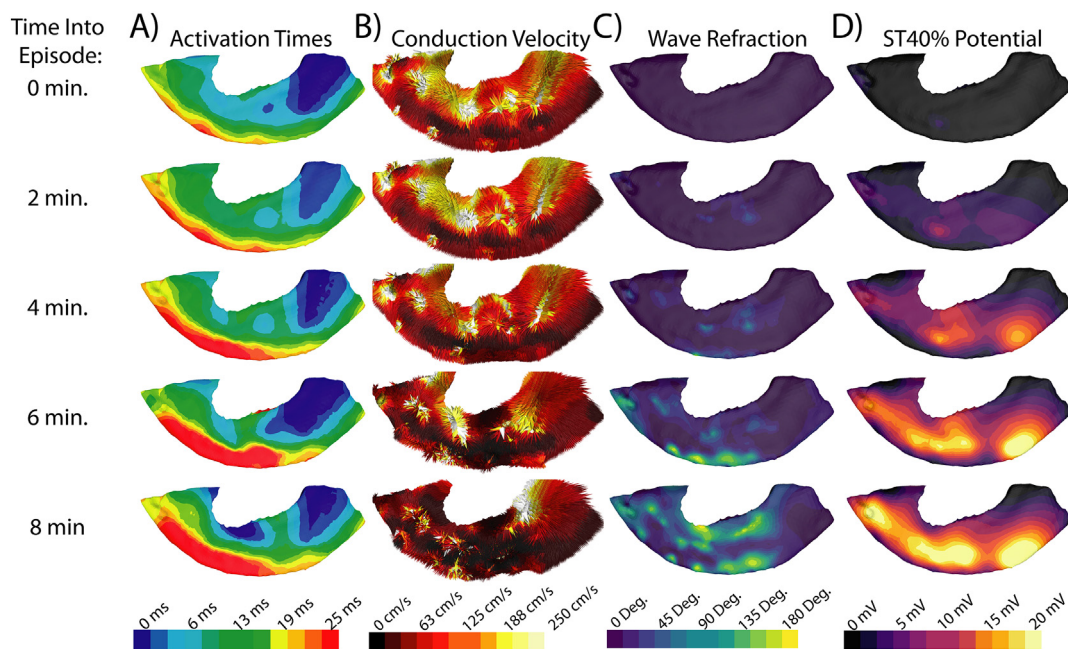


Fig. 2. The spatiotemporal progression of AT, CV, WR, and ST40%, within the needle envelope at five time instances over an 8-min episode of ischemia in Exp.#2. The colour bar for each measure is visualized below the visualized measure. **A)** Spatiotemporal progression of ATs over an episode of ischemia. **B)** Spatiotemporal progression of CV over an episode of ischemia. Note, the dense vector field generated using this method. **C)** Spatiotemporal progression of WR potential over an episode of ischemia. **D)** Spatiotemporal progression of ST40% potential over an episode of ischemia.

Statistical methods

All measures are reported as a median \pm standard deviation. To compare measures, we used two statistical tests: 1) a two-sample Kolmogorov-Smirnov test (KS-test) to evaluate the significance of the differences in distributions at two time points in the ischemic episode; and 2) a Student's *t*-test to test whether changes in the median across all considered episodes are significant. We evaluated the differences in the skewed distributions (preischemia and peak) using a two-sample KS-test with a significance threshold of 0.05. We also determined if the magnitude of change beyond zero was significant for these two measures and wave refraction (WR). We determined significance using a Student's *t*-test with a threshold of 0.05. The same statistical analyses were performed on the stratified medians: the KS-test to evaluate whether each episodic change was significant, and the Student's *t*-test to evaluate if the ensemble of changes across all episodes was significant. Significance is visualized in each relevant figure using a green star.

Results

Global effects of acute ischemia

Fig. 3A and B show box plots of the median ST40% and CS changes between peak and control periods across all 20 episodes of ischemia. Fig. 3C shows two sample distributions of at control (purple) and the peak of the ischemic episodes (pink), these distributions are representative of the changes we typically see and come from two separate experiments. Fig. 3D shows the CS distributions for the same episodes. The median value (across all episodes) of ST40% moved from 1.4 ± 1.0 mV before ischemia to a peak of 5.6 ± 4.0 mV. At the same time, the median value of CS dropped from 48.4 ± 11.9 cm/s to 30.8 ± 13.3 cm/s. The green star indicates statistical significance.

In order to ensure the changes were significant beyond baseline in addition to the distributions being significantly different from one another, we performed a student *t*-test of the global change (the entire

needle envelope) in the median ST40%, CS, and WR across all episodes. The median global ST40% change was 4.1 ± 4.1 mV, the median global CS dropped 19.9 ± 10.2 cm/s, and the median global WR was 29.8 ± 18.7 (all three statistically significant).

Transmural stratification of ischemic changes

Fig. 4A and B show the median ST40% and CS changes between control and peak periods across the 20 episodes of ischemia stratified by transmural extent. Fig. 4C shows two sample distributions (same episodes as in Fig. 3) of ST40% at control (left) and peak of ischemia (right), stratified by transmural region. Fig. 4D shows the stratified CS distributions for the same episodes. The median ST40% increased from universally low values of 1.3 ± 1.1 mV for the subendocardium, 1.3 ± 1.0 mV for the midmyocardium, and 0.7 ± 0.8 mV for the subepicardium to similar peak values of 6.5 ± 4.3 mV for the subendocardium, 5.9 ± 5.2 mV for the midmyocardium, and 4.1 ± 3.0 mV for the subepicardium. The median CS values were more variable across the myocardial wall before ischemia, 71.9 ± 24.4 cm/s for the subendocardium, 54.0 ± 5.8 cm/s for the midmyocardium, and 43.0 ± 5.3 cm/s for the subepicardium. The effects of ischemia also varied with location, with the median CS values dropping to 37.1 ± 20.5 cm/s for the subendocardium, 26.5 ± 12.0 cm/s for the midmyocardium, and 30.5 ± 10.7 cm/s for the subepicardium. All global changes induced by ischemia showed statistical significance while significance across transmural regions was less consistent. Although the values of clearly changed in response to ischemia (Fig. 4A), they did not vary significantly across the myocardial wall thickness, i.e., among subendocardium, midmyocardium, and subepicardium (Fig. 4A and C). Conduction speed also changed (dropped) significantly with ischemia (Fig. 4B), however, the significant differences across the myocardial wall that were present at control, diminished almost completely at peak ischemia (Fig. 4B and D).

We also measured the average change from baseline to peak levels of ischemia to identify the significance of the change we are observing. ST40% varied very little across the transmural extent with no significant differences observed in the stratified changes. Changes in CS were

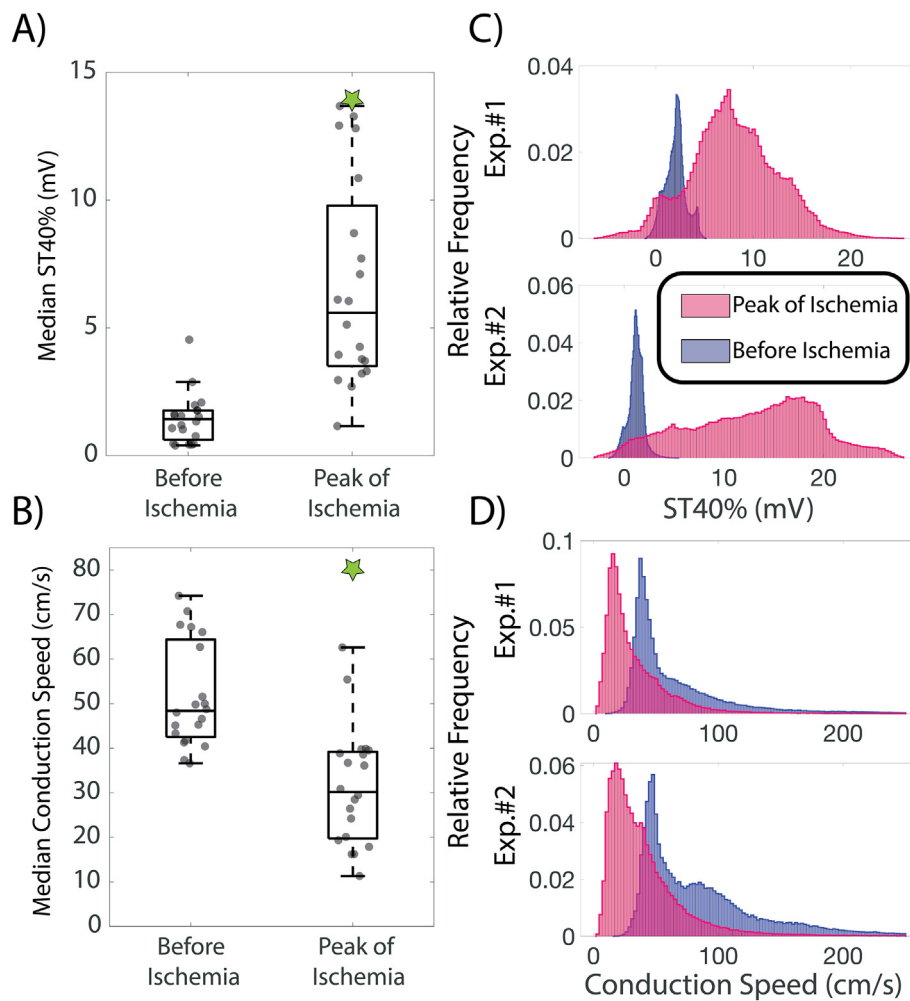


Fig. 3. Changes in CS and ST40% distributions between control and peak periods of the ischemic episodes. Significant difference between the preischemia and peak ischemia is indicated with a green star. **A)** The change in median ST40% across 20 episodes of ischemia. **B)** The change in median CS across 20 episodes of ischemia. **C)** Two sample ST40% distributions prior to the induction of ischemia (purple) and at the peak (pink) of the ischemic episodes. **D)** CS distributions prior to the induction of ischemia (purple) and at the peak (pink) of the ischemic episodes for the same episodes as in Panel C. (For interpretation of the references to colour in this figure legend, the reader is referred to the web version of this article.)

slightly more complicated. Whereas the largest absolute changes to CS appeared subendocardially, the median changes between the subendocardium and midmyocardium were not significantly different. However, the subepicardium did experience significantly lower amplitude changes to CS than either the subendocardium and midmyocardium. WR varied less across the transmural extent, and the stratified results show that the subendocardium had the highest median WR with $47.1 \pm 23.4^\circ$, followed by the subepicardium with $36.2 \pm 22.9^\circ$, and finally the midmyocardium with $28.3 \pm 19.9^\circ$. Only the difference between the subendocardium and the midmyocardium was significant. A Figure summarizing these average changes can be seen in the Supplemental Material.

Correlation between ischemic stress and conduction changes

Fig. 5A shows the global temporal correlation and the spatiotemporal correlation (STC) as well as the temporal correlation binned by transmural extent between ST40% and conduction slowing across 20 episodes of ischemia. The global temporal correlation was much higher than the STC, 0.91 ± 0.10 versus 0.59 ± 0.18 . The figure also shows the transmural heterogeneity in the temporal correlation, with the highest correlation in the midmyocardium (0.76 ± 0.21) followed by the subendocardium (0.54 ± 0.32) and finally the subepicardium (0.50 ± 0.19). To illustrate the high level of temporal correlation, Fig. 5B

shows four sample pairs of run-metric curves (one from each of four separate experiments) with elevation of ST40% and slowing of CS overlaid and time aligned.

Characterization of the biphasic response and temporal change

We characterized the average onset of major change in the ST40% and CS metrics from baseline conditions and the biphasic transitions and the results are summarized in Table 1. For a typical episode of ischemia, the progression of ST40% began 115 s into the ischemic episode, followed 65 s later by the progression phase of conduction slowing, with the biphasic response preceding the progression phase by 31 s.

In 12 of the 20 episodes of ischemia, we observed a paradoxical initial increase in the CS beyond baseline levels before subsequent slowing. This effect occurred most frequently in the subendocardium (9/12 episodes) and therefore we averaged only the subendocardium speeds in those 9 episodes in order to characterize the average increase in speed and duration of the period of acceleration. Fig. 6 shows an example of this response, where the subendocardium experienced a median increase in CS of 12.8 cm/s before subsequently dropping by 56 cm/s. On average, the speed accelerated 3.72 ± 3.41 cm/s before the onset of major change in conduction speed.

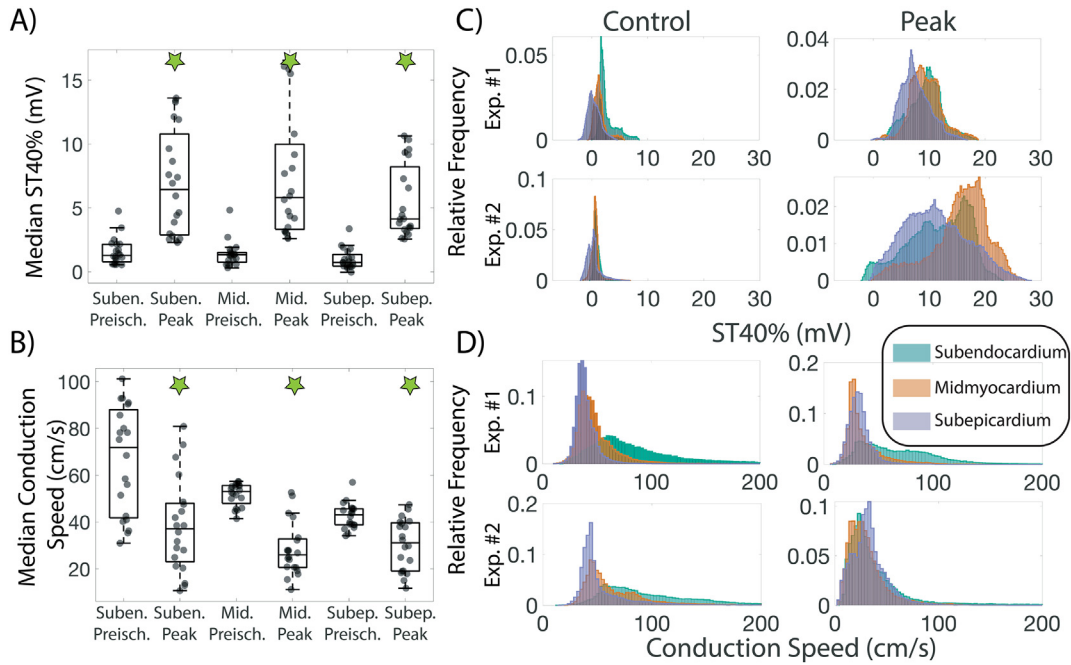


Fig. 4. Changes in CS and ST40% distributions between peak and control periods of the ischemic episodes stratified by transmural extent (subendo. = Green, midmyo. = Orange, and subepi. = Purple). The example distributions in C) and D) are the same as in Fig. 3. Significant difference between the preischemia and peak ischemia is indicated with a green star. **A)** The change in median across 20 episodes of ischemia stratified by transmural extent. **B)** The change in median CS across 20 episodes of ischemia stratified by transmural extent. **C)** ST40% distributions before and at peak ischemia for two sample episodes, stratified by transmural extent. **D)** CS distributions for the same episodes and same conditions. (For interpretation of the references to colour in this figure legend, the reader is referred to the web version of this article.)

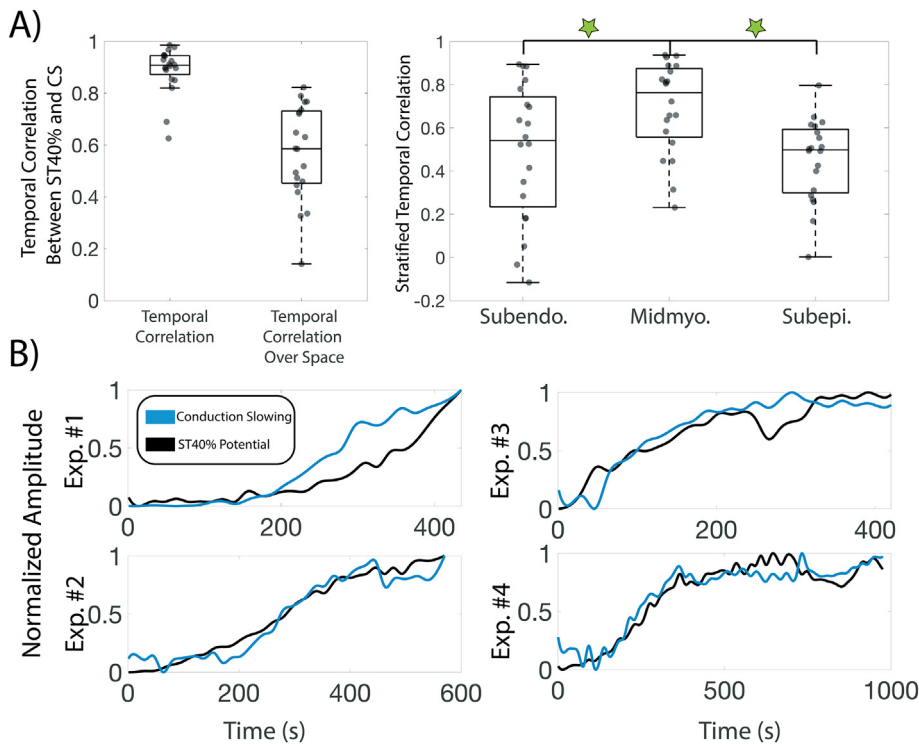


Fig. 5. Temporal correlation between ST40% and CS. **A)** Box plots showing the temporal correlation of ST40% and CS over 20 episodes of ischemia (left) and the temporal correlation over space binned by transmural extent (right). Significance in this figure is displayed between the midmyocardium and the subendocardium and subepicardium using a green star. No other distributions were significantly different from one another. **B)** Four sample run-metric curves showing overlaid ST40% (black) and conduction slowing (blue), one selected from each of the four experiments used in this study. Note, both curves are normalized and the CS run-metric is negated for the purposes of the correlation measure. (For interpretation of the references to colour in this figure legend, the reader is referred to the web version of this article.)

Table 1
The median \pm SE time point for the biphasic response and the onset of changes.

Metric being characterized	Biphasic onset \pm SE	Onset of major change \pm SE
ST40%	n/a	115 \pm 21 s
Conduction Speed	155 \pm 8 s	186 \pm 27 s

Discussion

This study has reported, for the first time to our knowledge, simultaneous estimations of ischemic stress and changes in the spread of excitation during episodes of acute ischemia in order to investigate the spatiotemporal relationship between these electrophysiological markers. We analyzed CS and ST40% changes over 20 episodes of graded ischemia across four canine experiments using a validated technique to reconstruct activation times and estimate CV/CS at resolutions limited only by the subject-specific, geometric model [8]. We applied these novel techniques to correlate and analyze the progression of ST40% and CS, and identified within the myocardium many of the features of altered physiology suspected of being arrhythmogenic.

Conduction velocity changes throughout an episode of acute myocardial ischemia

We observed significant changes in ST40%, CS, and wavefront direction within the putative perfusion zone during episodes of acute ischemia, changes that showed significant transmural heterogeneity, especially of CV. Although intramural measurements at the required density could include only part of the left ventricle, the qualitative findings with respect to the location and progression of ischemic ST40% values are supported by our previous studies [4,5]. Most notably, early development of acute ischemia is not bound to the subendocardium, rather regions of non-transmural ischemic stress are distributed throughout the myocardium, at least during the hyperacute phase

(< 15 min.) produced by partial coronary occlusions [4,5]. A major novel contribution of this study is that conduction speed is transmurally heterogeneous even before the induction of ischemia, with the fastest conduction in the subendocardium, followed by the midmyocardium and, finally, the subepicardium. The faster speeds seen at the subendocardium are most likely due to Purkinje-tissue junctions, which appear as multiple, discrete sites of almost simultaneous initiation of activation, resulting in very fast apparent spread of excitation (>100 cm/s). Surprisingly, the variability of conduction speeds at the peak of ischemia was reduced, i.e., they were more similar transmurally than before the onset of ischemia. We also found that the subepicardium experienced the smallest ischemia-induced reductions in CS. The subendocardial region showed the largest response to ischemia, both in terms of CS and the direction of propagation (refraction) of the wavefronts. This large subendocardial refraction—seen to a slightly lesser extent also in the subepicardium—may be explained by the lower safety factor associated with surface based propagation. This reduced safety factor makes the wavefront more susceptible to changes in anatomy or substrate (such as ischemic tissue) than a propagating wavefront with a high safety factor [22].

Changes in conduction velocity relative to identified ischemic zones

We examined the temporal progression of ischemic stress (ST40%) and correlated it with conduction slowing globally (temporal correlation) and within regions of the heart (spatiotemporal correlation). We observed generally high temporal correlation (correlation > 0.8), but surprisingly, the correlation between ST40% and CS progression varied across the myocardium. Previous studies, by us²³ and others^{9,24,24} have studied the changes in the spread of excitation during induced episodes of ischemia, however, typically without a temporally aligned metric of ischemic stress. For the first time to our knowledge, this study captured ST40% as a metric of ischemic stress simultaneously with CV, allowing measurements of correlations between both the global and regional time courses of these metrics. Our results indicate a close correlation

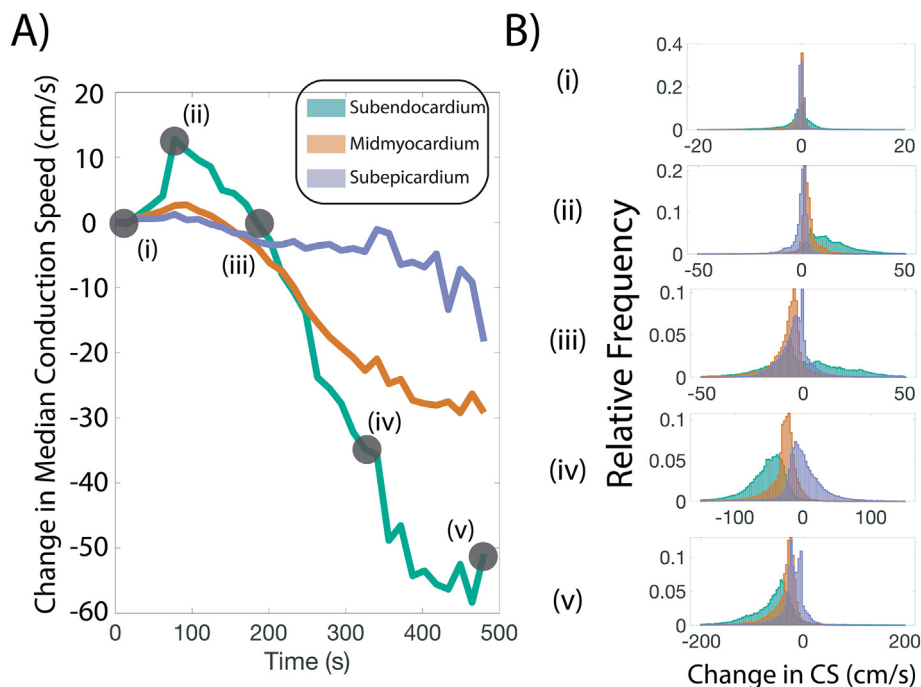


Fig. 6. An example run-metric of CS stratified by transmural extent during an episode of ischemia that shows a pronounced biphasic response in the temporal progression and the associated speed histograms normalized by probability. **A)** Stratified run-metric of CS during an episode of ischemia with five highlighted time points. **B)** Histogram of speed change from time points indicated in A). **i)** 15 s into the ischemic episode. **ii)** 90 s into the ischemic episode. **iii)** 195 s into the ischemic episode. **iv)** 345 s into the ischemic episode. **v)** 480 s into the ischemic episode.

between increased ischemic stress and decreased global conduction speed. We did capture two episodes in which ST40% increased modestly but without a concomitant drop in CS, which resulted in the only cases of temporal correlation dropping below 0.8. We also examined how the temporal correlation between ST40% and CS varied across space, captured with a metric we called 'spatiotemporal correlation' (STC). Here, we found far lower correlation. Such low values of STC suggest a complicated spatial relationship between changes in the ST-segment and the conduction speeds reflected in the QRS. Here, too, there was spatial heterogeneity, with relatively high STC in the midmyocardium (0.76) versus the subendocardium and subepicardium (0.54 & 0.50, respectively). Possible explanations for these findings include the presence of tissue boundaries (e.g., the blood pool at the) or due to relatively contiguous and continuous propagation in the midmyocardium.

The disparity between the high temporal correlation and moderate STC may also be explained by how we chose to represent the ischemic stress spatially via the ST40% metric. The spatial complexity that is not captured temporally could be due to the interplay between the propagating wave and the tissue experiencing ischemic stress. Furthermore, the activation sequence was found to have beat-to-beat variability during periods of high ischemic stress, variations not as pronounced in ST40% changes, which may further explain the low STC. A great deal of heterogeneity may be present in the AP changes throughout the myocardial wall, meaning ST40% may be more or less representative of the ischemic stress in some regions. We also measured notable and reproducible delays between the progression of ST40% and CS, as we have shown previously [20,23].

The biphasic response in conduction speed

A notable temporal response we observed was the paradoxical early appearance in some ischemic episodes of transient increases in CS before a rapid slowing. While this behavior has been suggested in previous studies based on biophysical theory and cellular experiments [25] it has never been documented volumetrically in the whole organ. During 12 of the ischemic episodes across all experiments, we observed a biphasic response in CS, for the most part isolated to the subendocardium. The initial increase in CS is most likely explained by the accumulation of extracellular potassium temporarily increasing the excitability of the tissue, as proposed by Elharrar et al. [25,26] Why this response appeared only in the subendocardium is unclear, but perhaps results from the heterogeneous distribution of ionic channel types across the myocardium; an additional factor could be the variability in cell types, such as Purkinje cells or the cardiomyocytes of the subendocardium that are particularly susceptible. Janse et al. [26] showed that the biphasic response was isolated to propagation along the longitudinal fiber orientation, therefore, it may be that the highly anisotropic early activation in the subendocardium has the highest volume fraction of longitudinal propagation. It is likely that biphasic responses occur throughout the wall (as Fig. 6 suggests), but that they do not contribute significantly enough to be seen in median CS values. The biphasic acceleration was on the same order of magnitude as the deceleration we observed subsequently, which may indicate an underlying monotonic accumulation of extracellular potassium concentration that elicits the biphasic response in excitability. Previous studies have suggested the biphasic response in CS is arrhythmogenic, particularly through reentrant type phenomena [27]. It is unclear whether this biphasic response contributes to arrhythmogenesis, however, it likely does disrupt the ordered (albeit complex) activation sequence in a manner that could be potentially arrhythmogenic.

Arrhythmogenesis of acute ischemia

The combination of spatial heterogeneity of CS and its temporal progression leads naturally to speculations related to the arrhythmogenesis that previous studies have shown occurs in early ischemia. Specific

features of altered spread of activation that we observed include: 1) the presence of slow- (<10 cm/s) and fast-response (>10 cm/s) regions in close spatial proximity [24]; 2) perturbations to the normal activation sequence [28]; and 3) the paradoxical biphasic response during early ischemia [26,27]. The time course of CS slowing observed intramurally agree with studies that measured prolongation of the QRS on the epicardium [29]. Furthermore, the QRS widening (a surrogate of reduction in CS in the myocardium) on the epicardium was associated with subsequent development of ventricular fibrillation [30]. In the early phases of ischemia it is thought that the primary source of CS changes is a diminished fast-response of Na-channel activity; followed in the latter phases by eventual complete elimination of the Na currents and nearly complete reliance on the slow response, as studied by Cranefield et al. [24] The switch from the fast to the slow response occurs when CS falls below about 10 cm/s, resulting in a dramatic decrease in the safety factor and potential intermittent excitability, which are known to be arrhythmogenic [24]. Ischemic stress also diminishes the electrical coupling prevalent under normal physiological conditions, disrupting the syncytial nature of the myocardial coupling and allowing for sharp changes in the CS, which we observed throughout the needle envelope. Furthermore, the reduced safety factor due to ischemia can result in conduction blocks and in dramatic changes in the wavefront direction, as was shown by the spatial wave refraction (WR), with 180 degrees of refraction within 5 mm of the unperturbed wavefront. These conditions establish the arrhythmogenic nature of reentry that we associate with acute ischemia. In several episodes and across all experiments, we observed cases of conduction speeds indicative of the fast and slow-response throughout the needle envelope as well as large WR at the anatomical boundaries.

The propagation sequence of the heart under sinus rhythm, although complex, is surprisingly repeatable, and we saw minimal beat-to-beat variability in refraction between sequential beats. This beat-to-beat similarity was disrupted by ischemic stress and the propagation sequence changed from one beat to another. Studies by Costa et al. and others have shown that disruptions to the wavefront of the typical activation sequence are particularly arrhythmogenic, as the propagation occurs counter to the AP duration gradient [2,24,28]. Whether the initial arrhythmogenesis is due to excitation generated via injury currents or reentry, the two predominant theories behind arrhythmogenesis in ischemia, remains to be determined; however, the observed slow-response and large heterogeneous WR establish favorable conditions for either scenario. Of course, such speculation must also include information about repolarization, the parameters of which are also available from our studies. Our ongoing studies will seek to identify the mechanistic underpinnings of ischemia-related arrhythmogenesis.

Limitations

Our study shares the limitation of all mapping studies in that spatial sampling and coverage are a compromise between achievable electrode densities and maintaining a viable, living organ under physiological conditions. Our sampling was relatively dense in the radial direction (1.5–1.7 mm), ideal for studying transmural gradients. Sampling in orthogonal directions was more limited (1–2 cm), making spatial examination in these directions more prone to error. However, our validation studies suggest that even in these relatively sparsely sampled regions, the CV can be estimated with high fidelity [20]. Furthermore, we were sampling only a portion of the ventricular myocardium and, therefore, cannot comment on changes in CS outside the needle envelope. Our recordings were limited to extracellular sampling, which limits our analysis to electrograms without directly examining the action potentials themselves. Finally, we specifically avoided prolonged episodes of arrhythmia in the experiments because of the threat of subsequent fibrillation and premature death of the animal. As a result, the discussion of arrhythmogenesis is more speculative than it will be from future studies.

Conclusion

This study is the first to report, from experiments, volumetric conduction speed changes during episodes of acute ischemia. We showed that conduction speed changes are temporally correlated to ischemic severity, and we illustrated the biphasic response long-proposed in cellular studies. Furthermore, our results suggest only a moderate spatio-temporal correlation between ischemic stress and conduction slowing, suggesting a more complex relationship between ischemic stress and changes to CS with significant slowing observed on the periphery of the region of ischemic stress.

Acknowledgements

This project was supported by the National Institute of General Medical Sciences of the National Institutes of Health under grant number P41 GM103545-18 and the Nora Eccles Treadwell Foundation at the Cardiovascular Research and Training Institute (CVRTI) funded the experiment data collection.

Appendix A. Supplementary data

Supplementary data to this article can be found online at <https://doi.org/10.1016/j.jelectrocard.2021.03.004>.

References

- [1] Janse M, Kleber AG. Electrophysiological changes and ventricular arrhythmias in the early phase of regional myocardial ischemia. *Circ Res.* 1981;49(5):1069–81.
- [2] Zipes DP, Wellens HJ. Sudden cardiac death. *Circulation.* 1998;98(21):2334–51.
- [3] Elharrar V, Zipes D. Cardiac electrophysiologic alterations during myocardial ischemia. *Am J Physiol Heart Circ Physiol.* 1977;233(3):H329–45.
- [4] Zenger B, Good WW, Bergquist JA, Burton BM, Tate JD, Berkenbile L, et al. Novel experimental model for studying the spatiotemporal electrical signature of acute myocardial ischemia: a translational platform. *Physiol Meas.* 2020;41(1):015002.
- [5] Aras K, Burton B, Swenson D, MacLeod R. Spatial organization of acute myocardial ischemia. *J Electrocardiol.* 2016;49(3):323–36.
- [6] Janse MJ, Van Capelle FJ, Morsink H, Kleber AG, Wilms-Schopman F, Cardinal R, et al. Flow of “injury” current and patterns of excitation during early ventricular arrhythmias in acute regional myocardial ischemia in isolated porcine and canine hearts. Evidence for two different arrhythmogenic mechanisms. *Circ Res.* 1980;47(2):151–65.
- [7] Elharrar V, Zipes D. Cardiac electrophysiologic alterations during myocardial ischemia. *Am J Physiol Heart Circ Physiol.* 1977;233(3):H329–45.
- [8] Good WW, Erem B, Coll-Font J, Zenger B, Bergquist JA, Brooks D, et al. Characterizing the transient electrocardiographic signature of ischemic stress using laplacian eigenmaps for dimensionality reduction. *IEEE Transactions in Biomedical Engineering; 2020 In Preparation.*
- [9] Kleber AG, Janse MJ, Wilms-Schopman F, Wilde A, Coronel R. Changes in conduction velocity during acute ischemia in ventricular myocardium of the isolated porcine heart. *Circulation.* 1986;73(1):189–98.
- [10] Bayly PV, KenKnight BH, Rogers JM, Hillsley RE, Ideker RE, Smith WM. Estimation of conduction velocity vector fields from epicardial mapping data. *IEEE Trans Biomed Eng.* 1998;45(5):563–71.
- [11] Barnette AR, Bayly PV, Zhang S, Walcott GP, Ideker RE, Smith WM. Estimation of 3-d conduction velocity vector fields from cardiac mapping data. *IEEE Trans Biomed Eng.* 2000;47(8):1027–35.
- [12] Taccardi B, Punske BB, Macchi E, MacLeod RS, Ershler PR. Epicardial and intramural excitation during ventricular pacing: effect of myocardial structure. *Am J Physiol Heart Circ Physiol.* 2008;294(4):H1753–66.
- [13] Cantwell CD, Roney CH, Ng FS, Siggers JH, Sherwin S, Peters NS. Techniques for automated local activation time annotation and conduction velocity estimation in cardiac mapping. *Comput Biol Med.* 2015;65:229–42.
- [14] Aras K, Burton B, Swenson D, MacLeod R. Sensitivity of epicardial electrical markers to acute ischemia detection. *J Electrocardiol.* 2014;47(6):836–41.
- [15] Aras K, Burton B, Swenson D, MacLeod R. Spatial organization of acute myocardial ischemia. *J Electrocardiol.* 2016;49(3):689–92.
- [16] Rodenhauer A, Good WW, Zenger B, Tate J, Aras K, Burton B, et al. Pfeifer: pre-processing framework for electrograms intermittently fiducialized from experimental recordings. *J Open Source Softw.* 2018;3:472.
- [17] Bayer J, Prassl AJ, Pashaei A, Gomez JF, Frontera A, Neic A, et al. Universal ventricular coordinates: a generic framework for describing position within the heart and transferring data. *Med Image Anal.* 2018;45:83–93.
- [18] Bergquist JA, Good WW, Zenger B, Tate JD, RS MacLeod. GRÖMeR: A pipeline for geodesic refinement of mesh registration. *Lecture Notes in Computer Science. Functional Imaging and Model of the Heart (FIMH)*, Springer Verlag; 2019. p. 37–45.
- [19] Neic A, Gsell MA, Karabelas E, Prassl AJ, Plank G. Automating image-based mesh generation and manipulation tasks in cardiac modeling workflows using meshtool. *SoftwareX.* 2020;11:100454.
- [20] Good WW, Gillette K, Bergquist JA, Zenger B, Rupp LC, Tate J, et al. Estimation and validation of cardiac conduction velocity and wavefront reconstruction using epicardial and volumetric data. *IEEE Transactions in Biomedical Engineering; 2020 In Preparation.*
- [21] Taccardi B, Punske B, Macchi E, MacLeod R, Ershler P. Epicardial and intramural excitation during ventricular pacing: effect of myocardial structure. *Am J Physiol.* 2008; 294(4):H1753–66.
- [22] Kleber AG, Rudy Y. Basic mechanisms of cardiac impulse propagation and associated arrhythmias. *Physiol Rev.* 2004;84(2):431–88.
- [23] Good WW, Erem B, Zenger B, Coll-Font J, Brooks DH, MacLeod RS. Temporal performance of laplacian eigenmaps and 3d conduction velocity in detecting ischemic stress. *J Electrocardiol.* 2018;51(6):S116–20.
- [24] Cranefield PF, Wit AL, Hoffman BF. Conduction of the cardiac impulse: iii. Characteristics of very slow conduction. *J Gen Physiol.* 1972;59(2):227–46.
- [25] Elharrar V, Foster PR, Jirak TL, Gaum WE, Zipes DP. Alterations in canine myocardial excitability during ischemia. *Circ Res.* 1977;40(1):98–105.
- [26] Janse M, Kleber A, Capucci A, Coronel R, Wilms-Schopman F. Electrophysiological basis for arrhythmias caused by acute ischemia: role of the subendocardium. *J Mol Cell Cardiol.* 1986;18:339–55.
- [27] Jie X, Trayanova NA. Mechanisms for initiation of reentry in acute regional ischemia phase 1b. *Heart Rhythm.* 2010;7(3):379–86.
- [28] Costa CM, Neic A, Gillette K, Porter B, Gould J, Sidhu B, et al. Left ventricular endocardial pacing is less arrhythmogenic than conventional epicardial pacing when pacing in proximity to scar. *Heart Rhythm.* 2020;17(8):1262–70.
- [29] Romero D, Ringborn M, Demidova M, Koul S, Laguna P, Platonov PG, et al. Characterization of ventricular depolarization and repolarization changes in a porcine model of myocardial infarction. *Physiol Meas.* 2012;33(12):1975.
- [30] Demidova MM, Martín-Yebra A, van der Pals J, Koul S, Erlinge D, Laguna P, et al. Transient and rapid qrs-widening associated with a j-wave pattern predicts impending ventricular fibrillation in experimental myocardial infarction. *Heart Rhythm.* 2014;11(7):1195–201.